Available online at www.sciencedirect.com
SCIENCE DIRECT®
Journal of Sound and Vibration 266 (2003) 493–514
JOURNAL OF SOUND AND VIBRATION
www.elsevier.com/locate/jsvi

Discrete element modelling for process simulation in agriculture

E. Tijskens*, H. Ramon, J.De Baerdemaeker

Laboratory for Agro-Machinery and Processing, Department of Agro-Engineering and -Economics, Catholic University Leuven, Kasteelpark Arenberg 30, 3001 Leuven, Belgium

Received 13 January 2003

Abstract

This paper presents an overview of discrete element modelling (DEM) as a modelling technique for granular assemblies. It focusses on DEM for agricultural products and processes and discusses important algorithmic and physical issues connected to this domain. Existing applications in the literature are reviewed and an overview of ongoing DEM applications in the Laboratory for Agro-Machinery and Processing is presented.

1. Introduction

Granular materials abound in nature, in industry and particularly in the agro-industry, where nearly every harvested product goes through one or more granular stages during the handling chain from harvest to consumer. Granular matter is generally thought of as a simple and unsophisticated form of matter, being just an assembly of discrete macroscopic grains. However, this is a gross misconception which is probably due to the ubiquitous nature of granular materials. Already during early childhood, while playing with sand, we learn about the different properties of dry (flow) and wet sand (stability, arching) and how shaking a sieve brings the bigger sea shells to the surface (segregation). Engineers dealing with bulk handling systems realize very well that granular materials are extremely difficult to handle with respect to flow and mixing [1–13]. Estimates are that about 40% of the capacity of industrial plants are wasted because of bulk handling problems [14,15]. In the agro-industry many problems are related to product damage due to impact or vibration during processes like harvesting, transport in palloxes, sorting, bulk

*Corresponding author. Tel. +32-16-32-8595; fax: +32-16-32-8590.
E-mail address: engelbert.tijskens@agr.kuleuven.ac.be (E. Tijskens).

0022-460X/$ - see front matter © 2003 Elsevier Ltd. All rights reserved.
doi:10.1016/S0022-460X(03)00581-9

storage, etc. e.g., bruising of apples is reported as a serious quality threat [16]. The annual production of apple in Belgium is about 512 000 tonnes, of which about one-sixth is unsuitable for sale due to bruising. Subcutaneous tissue discoloration in potatoe tubers is also caused by impact (static and dynamic) and is reported be responsible for losses up to 20% [17,18]. Softer products, like tomatoes, suffer from puncture due to impact by the harder stem. Losses amount to 10%.

During the last decade granular materials have drawn interest, not only to engineers [8,10,19] trying to solve practical problems, but also to physicists, realizing that granular matter pose numerous interesting questions of fundamental nature [8,10,13,20–22] and to researchers in the scientific computing concerned with modelling granular systems [23–30]. Solving practical problems in real life requires expert knowledge in each of these domains.

The paper is organized as follows. In Section 2 the physical and mathematical setting of DEM is explained and the basic DEM algorithm is given. The subsequent Sections 3–6 discuss the respective components of this algorithm in some detail stressing some issues of particular importance when dealing with agricultural products. Section 7 reviews reported applications in agriculture and discusses current DEM projects in the Laboratory for Agro-Machinery and Processing. Finally, some conclusions are drawn.

2. Discrete element modelling

Discrete element modelling was originally pioneered by Cundall and Strack [31] and Cundall [32] in the field of rock mechanics. DEM is essentially a numerical technique to model the motion of an assembly of particles interacting with each other through collisions. As such it is quite comparable to molecular dynamics (MD) [33], from which it borrows some techniques and experience. Both techniques sum up the forces acting on the particles and integrate Newton's equations of motion to obtain velocity and position at the next time step. In doing so, the technique describes the path of every particle in the assembly as time proceeds. Notable differences with molecular dynamics are the fact that in DEM the particles are not point masses as in MD, but necessarily have a finite extent in 2 or 3 dimensions. This implies the possibility of rotational degrees of freedom. Also the nature of the forces acting on the particles is different. In the first place, contrary to interaction forces in MD, contact forces in granular systems are not conservative due to the inelastic nature of collisions and the presence of friction forces on contact surfaces. As a consequence, energy and momentum are dissipated, i.e., transferred to internal degrees of freedom of the particles. Furthermore, interaction forces between atoms and molecules are determined by continuous long-range and/or short-range potentials, whereas in granular systems both the contact force and its gradient may show discontinuities depending on the contact force model that is applied. Finally, as contact forces act only on particles in mutual contact, a contact detection algorithm is required in DEM programs, something which is absent in MD programs.

Physically, particles in a DEM problem are approximated as *rigid bodies* and the contacts between them as *point contacts*. In reality, most particles are of course more or less deformable, and this is accounted for by allowing the particles to overlap slightly. As overlapping particles can of course only exist in a computer model, this overlap is termed *virtual overlap*, δn. The forces resulting from a contact between two particles are related to their virtual overlap by a *contact*

force model. Mathematically, a DEM problem is formulated as a non-linear system of coupled ordinary differential equations (ODE) formed by Newton's equations of motion for each individual particle:

$$m_i\mathbf{a}_i = \mathbf{G}_i + \sum_c \mathbf{F}_{ci},$$
$$\mathbf{I}_i\boldsymbol{\alpha}_i = \mathbf{H}_i + \sum_c \mathbf{r}_{ci} \times \mathbf{F}_{ci}, \quad i = 1, \ldots, N. \tag{1}$$

Here, $\mathbf{a}_i$ and $\boldsymbol{\alpha}_i$ are the translational and rotational acceleration of the ith particle and m_i and $\mathbf{I}_i$ designate its mass and inertia tensor. $\mathbf{G}_i$ and $\mathbf{H}_i$ are, respectively, the body force and moment acting on the ith particle. Most frequently, one has

$$\mathbf{G}_i = \begin{bmatrix} 0 \\ 0 \\ -m_i g \end{bmatrix}, \quad \mathbf{H}_i = \begin{bmatrix} 0 \\ 0 \\ 0 \end{bmatrix}. \tag{2}$$

In addition the particle experiences contact forces $\mathbf{F}_{ci}$ arising from contacts with neighbouring particles which is the contact force acting on the particle due to the cth contact and $\mathbf{r}_{ci} = \mathbf{r}_c - \mathbf{r}_i$ is the position vector of that contact relative to the particle's center of mass. The ODEs in system (1) are coupled because the contact force $\mathbf{F}_{ci}$ depends on the relative position and velocity of the particles in contact with particle i. Non-linearities arise because contact forces act only between particles in contact. Even in the simplest case of a normal contact force modelled by a linear spring

$$F_{ci} = k\xi_c, \quad \xi_c \geqslant 0 \tag{3}$$

(k is the spring constant and ξ_c the virtual overlap of contact c) the problem becomes non-linear because in the case of dry contacts F_{ci} has to vanish for $\xi < 0$. A more correct statement of the contact law (3) would therefore be

$$F_{ci} = \max(0, k\xi_c), \quad \delta n_c \in \mathbb{R}. \tag{4}$$

The contact non-linearity is illustrated in Fig. 1. A similar non-linearity arises in the case of dry friction. According to Coulomb's law of dry friction, a normal force implies a tangential friction force:

$$F^{fric} \leqslant \mu_s F_n \quad (static), \tag{5}$$

$$F^{fric} = \mu_d F_n \quad (dynamic). \tag{6}$$

The $\leqslant$ sign in Eq. (6) means that for the case of static friction (vanishing tangential velocity, $\dot{x}_\tau$), F^{fric} compensates exactly the (unknown) external tangential force F_τ^{ext} applied to the contact, so that $\dot{x}_\tau = 0$ is maintained. If $F_\tau^{ext} > \mu_s F_n$, the dynamic regime is entered, and Eq. (6) applies. Note that Eqs. (5) and (6) describe only the magnitude of the friction force F^{fric}. Its sign is given by

$$\mathrm{sgn}(F^{fric}) = -\mathrm{sgn}(F_\tau^{ext}). \tag{7}$$

The situation is depicted graphically in Fig. 2. Finally, nonlinearities may arise because the contact force model itself is non-linear. For example the Hertz contact law dictates that the contact force between two spherical elastic bodies is proportional to the 3/2th power of the virtual

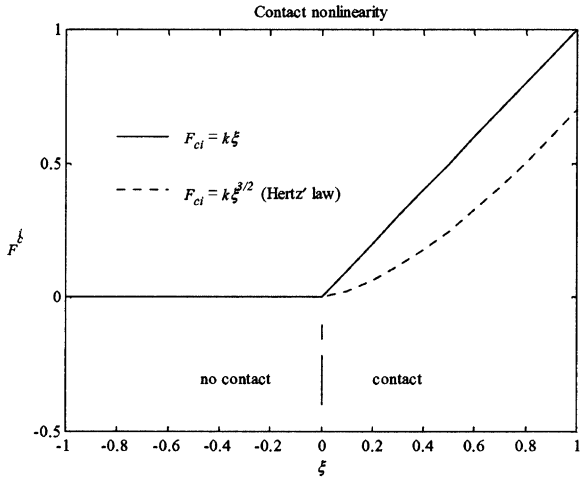

Fig. 1. The contact nonlinearity for a normal contact force modeled by a linear spring (3) and by the Hertz law (arbitrary units).

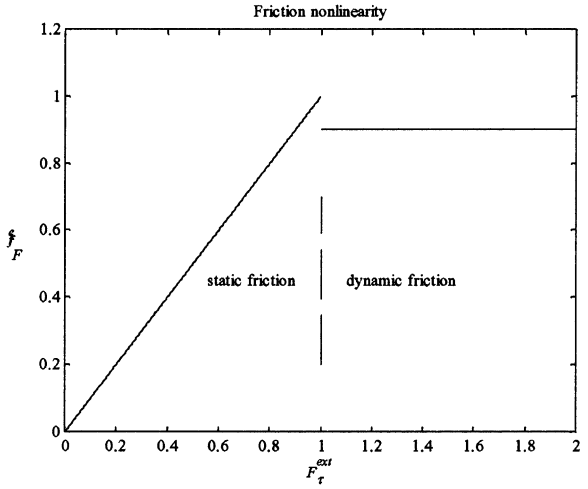

Fig. 2. Dry friction nonlinearity: friction force F^{fric} according to Eqs. (5) and (6) as a function of the external tangential force, F_τ^{ext}, applied to the contact for a fixed normal force, F_n (arbitrary units).

overlap (see Fig. 1).

$$F_{ic} = k\xi_c^{3/2}. \tag{8}$$

The typical DEM algorithm is then organized as follows:

1. Initialize the system. Since the ODE system (1) is a system of second-order differential equations, two initial conditions are required for every degree of freedom, i.e., for every

particle the translational and rotational position and velocity at time $t = 0$ must be fixed. Also the time step (Δt) is initialized.

2. Determine all contacts in the system at the current time. This usually proceeds in two steps:
   2.1. *Spatial sorting*: in principle, every particle may be in contact with every other particle, so the size of the set of all possible contacts is $N(N-1)/2 = O(N^2)$. Spatial sorting constructs a set of possible contacts which is smaller than $N(N-1)/2$, by including only particle pairs which cannot be falsified immediately. The ultimate goal is to obtain a set with a size $O(N)$.
   2.2. *Spatial resolution* applies a decisive test to every element of the set of possible contacts after spatial sorting. Its outcome is the set of actual contacts.

   Spatial sorting is necessary to make the contact detection step run in $O(N)$ time rather than $O(N^2)$.
3. Compute the contact forces for every actual contact.
4. Assemble the forces and moments acting on each individual particle in Newton's equations of motion (1).
5. Integrate Newton's equations of motion (1) over the time step Δt to obtain updated positions and velocities, and advance the time: $t = t + \Delta t$.
6. If the simulation is not finished, restart at step 2.

The algorithm contains several non-trivial steps, most of which depend on the method used to describe the shape of the particles. This will be considered first.

3. Shape representation and spatial resolution

Geometric model particles are defined by describing their surface. A detailed taxonomy of geometric models has been presented by Lin and Gottschalk [34]. Most frequently used are implicit surfaces, parametric surfaces and polygonal models.

An *implicit surface* is defined by a mapping f from space to the real numbers $f : \mathbb{R}^d \to \mathbb{R}$ as the set of points of space $\mathbf{x}$ for which $f(\mathbf{x}) = 0$. In the context of granular systems particles are usually closed manifolds, i.e., they have a well-defined inside and outside (walls or machine parts may constitute exceptions to this). Implicit surfaces automatically satisfy this requirement.

Spheres, described by

$$f(x, y, z) = x^2 + y^2 + z^2 - r^2 = 0, \tag{9}$$

are typical and most attractive examples because the contact between pairs of spheres can be easily verified as

$$\delta n \equiv (r_i + r_j) - \|\mathbf{x}_i - \mathbf{x}_j\| > 0. \tag{10}$$

Here $\mathbf{x}_i$ is the position of the centre of the ith sphere, and r_i its radius. The quantity δn is called the *virtual overlap* and is intimately connected to analytical contact force models (see Section 5).

The hyper-quadric surface is a generalization of the sphere which is also often used in DEM:

$$\left(\frac{x}{a}\right)^m + \left(\frac{y}{b}\right)^n + \left(\frac{z}{c}\right)^p - 1 = 0. \tag{11}$$

The larger the powers, the sharper the edges of the particle become, and the larger a (resp. b, c), the larger the particle becomes in the x direction (resp. y, z). Spatial resolution algorithms have been devised for general curved surfaces [35] and for hyper-quadric surfaces in particular [27]. The test is based on the solution of a non-linear algebraic system with real solutions if the surfaces intersect, and complex solutions otherwise. Obviously, spatial resolution is far more expensive than for spheres.

Surfaces can also be represented parametrically. *Parametric surfaces* are defined by a mapping from some subset of the plane to space $f : \mathbb{R}^{d-1} \to \mathbb{R}^d$. Unlike implicit surfaces they do not generally define closed manifolds. Typical examples are surfaces represented by non-uniform rational B-splines (NURBs) [36] or Bezier patches [37]. Contact tests proceed as described for hyper-quadric surfaces.

Finally, a particle's surface can be represented as a set of connected polygons, typically triangles. Such *polygonal models* are very versatile and widely used in computer graphics and modelling, but their non-smooth nature makes them somewhat less attractive for discrete contact force models. The intersection of a pair of polygons however can be easily verified. Let $\mathbf{n}_k$ be the normal of the kth polygon P_k and $\pi_{\mathbf{n}_k}(P_l)$ be the orthogonal projection of polygon P_l onto $\mathbf{n}_k$. Then both polygons intersect iff

$$\pi_{\mathbf{n}_k}(P_l) \subset \pi_{\mathbf{n}_k}(P_k) \tag{12}$$

and

$$\pi_{\mathbf{n}_l}(P_k) \subset \pi_{\mathbf{n}_l}(P_l). \tag{13}$$

If either one of these conditions is false the polygons are disjoint, and the other condition may be skipped. Note that $\pi_{\mathbf{n}_k}(P_k)$ is just a single point, as $\mathbf{n}_k \perp P_k$. Hence, as soon as the projection of two vertices of P_l lie on either side of this point, the test yields true and the remaining vertices of P_1 need not to be tested. Although the contact test for a pair of polygons is cheap, it should be realized that 3D particles can consist of quite large numbers of polygons. Checking the intersection of a pair of polygonal particles by checking all possible polygon pairs is not a realistic option. Some pruning mechanism is needed. For example, one can try to cut down the cost of spatial resolution by postponing the execution of a decisive test, and running some cheap tests which can further restrict the number of possible contacts in order to reduce the number of decisive tests. Various algorithms of this sort have been devised by the computer graphics and computational geometry community. Most of them share the fact that the particles are built up hierarchically as a tree. Each node in the tree stands for a subset of the particle, and has a bounding volume associated with it. Cheap intersection tests on these bounding volumes must allow one to prune the tree quickly to decide whether a decisive test is necessary or not. This principle is most commonly used for polygonal particles but can also be applied for implicit or parametric surfaces. Typical examples of bounding volumes are spheres, axis-aligned bounding box (AABBs), oriented bounding box (OBBs), k-dops (discrete oriented polytopes), spherical shells (for details see Refs. [38–40]). Note that the pruning of the tree is in fact a spatial sorting problem on a lower level, where the bounding volumes play the role of the particles. Consequently, some of the principles of the following section are reapplied.

It should be clear by now that, except for spheres, contact tests are expensive. This provided a rationale for composing particles of general shape as a rigid collection of overlapping spheres.

This idea has been worked out in detail by Favier et al. [41], Kremmer and Favier [42] and Abbaspour et al. [43] for axisymmetric particles. A comparison with other methods capable of representing general shapes is however still lacking.

4. Contact detection

Contact detection, or *collision* detection as it is called in computer graphics and computational geometry research, is a two-step process. The two steps are also known as *spatial sorting* and *spatial resolution*, respectively [23]. During spatial sorting the set of theoretically possible contacts is restricted. Next, spatial resolution subjects the restricted set of possible contacts to a decisive test. The exact form of this test depends on the shape representation of the particles participating in the possible contact (see Section 3). Thus, the cost of contact detection can be analyzed as the cost of spatial sorting plus the product of the size of this set and the cost of the spatial resolution test.

Several contact detection algorithms have been described in literature either related to DEM [24,30,44,45] or computer graphics and computational geometry research [34,46–51]. A most trivial contact detection algorithm is not to restrict the set of theoretically possible contacts at all, and simply subject every distinct pair of particles to the contact test. This results in $N^2(N-1)$ contact tests. Its quadratic complexity in the number of particles N identifies it as a very inefficient algorithm. Nevertheless, it can be useful for validating new contact detection algorithms, or in cases where the number of particles is small and the cost of the simulation is determined by components other than contact detection.

Spatial decomposition techniques rely on dividing the space occupied by the particles, so that one needs to check for contact between pairs of particles that are in the same or nearby cells of the decomposition. Two algorithms widely used in DEM do this decomposition by overlying the problem domain with a regular grid of cubic cells [52,53]. In the *grid search algorithm* [30,54,55] the size of a cell is determined so that every cell can accommodate at most one particle, i.e., the cell size is given by $\sqrt{2}(R_{min}-\varepsilon)$, where R_{min} is the radius of the smallest particle and ε is the maximum overlap that can occur. The set of possible contacts then contains only pairs of particles in cells no further apart than $2R_{max}$. This reduces the complexity to $O(NR_{max}^d/R_{min}^d)$, where d is the dimension of the problem space. In the *linked list algorithm* [30,56,57] a cell size of $2R_{max}$ is taken, so that particle pairs in contact can only reside in the same cell or in neighbouring cells. Here, the complexity is $O(N[(2R_{max})^d\rho]^2)$, with ρ the average particle density. The name of the algorithm is taken from the fact that a linked list is a very convenient data structure for remembering the particles residing in a particular cell. A deficiency of both algorithms is that, when the grid is implemented as an array, they may waste too much storage when the particle density becomes zero in large parts of the problem domain. This can be overcome by implementing the grid as a hash table. Vankreveld et al. [58] have shown that storage requirements are then independent of the size of the problem domain and of order $O(N)$. Point location queries can be performed in constant time. The grid search algorithm and the linked list algorithm both yield an optimal complexity of order $O(N)$, provided that the particles in the simulation are roughly uniform in size. Performance quickly degrades as the assembly's scale factor R_{max}/R_{min} becomes larger than unity, or as the number of particles per cell $(2R_{max})^d\rho$ becomes larger than unity. The presence of

a few large particles in the assembly can cause a dramatic performance deterioration. This is a major shortcoming.

Iwai et al. [30] report several variants of the linked list and grid search methods which remedy the performance degradation due do the presence of particles of different size. They noticed that the search radius can be allowed to vary as a function of the particle for which candidate particles are sought. In particular it is sufficient to search for candidate particles within a radius $2r_i$ of the ith particle. A small particle will of course fail to detect the contact with a larger particle, but it will be detected by the larger particle. By allowing the search radius to depend on the radii of both particles $r_i + r_j$ the performance can be improved even further. This can be achieved by introducing different grids of increasing cell size (layers) and putting the larger particles in the larger grids. In order to save memory space the different layers are implemented as hash tables.

The Octree method [59,60] is a spatial decomposition techniques that also avoids storing empty cells, and can deal with assemblies in which the ratio R_{max}/R_{min} departs seriously from unity. It derives from a binary search and sort. Constructing and searching the Octree can be done in $O(N\log N)$ provided it is balanced. Maintaining the balance throughout the simulation is, however, not easily accomplished.

Contact detection algorithms have been designed based on algorithms which are in general expensive, i.e., not of $O(N)$, but which become efficient for the special case presented by contact detection due to *spatial* and *temporal coherence*, a term used to indicate that the configuration of the particles undergoes only minor changes from time step to time step [51].

Ferrez et al. [26] and Müller [61] describe a gridless contact detection algorithm based on *dynamic triangulation*. A Delaunay triangulation is constructed with the centres of the particles as vertices. Although the construction of a Delaunay triangulation is in general a time consuming procedure, maintaining the triangulation over the time steps of the simulation can be done efficiently due to spatial and temporal coherence. The technique has no problems with large scale factors, but is restricted to spheres or 2D polygons.

Spatial heapsort is a gridless algorithm that relies on sorting the particles according to their co-ordinates on d global axes with the heapsort sorting algorithm. Only pairs of particles whose projections overlap on all axes are candidates for a contact test. It has been reported to be superior to Octree methods [23,24]. Heapsort [62] as a general sorting algorithm is $O(N\log N)$ for unsorted lists but the required changes at every time step are small due spatial and temporal coherence.

5. Contact force models

Contact forces are typically decomposed into normal and tangential components, with respect to the contact surface. For simplicity, the discussion is restricted to spherical particles in three dimensions. Schäfer et al. [63] present an overview of contact force model in physics.

The normal direction pointing from the contact surface to particle i is given by

$$\mathbf{n}_{ij} = (\mathbf{x}_i - \mathbf{x}_j)/|\mathbf{x}_i - \mathbf{x}_j| \tag{14}$$

and the tangential direction by

$$\boldsymbol{\tau}_{ij} = \mathbf{v}_{ij}/|\mathbf{v}_{ij}|, \tag{15}$$

where $\mathbf{v}_{ij}$ is the relative surface velocity:

$$\mathbf{v}_{ij} = \mathbf{v}_i - \mathbf{v}_j - [(\mathbf{v}_i - \mathbf{v}_j)\cdot\mathbf{n}_{ij}]\mathbf{n}_{ij} + \mathbf{r}_{ci}\times\boldsymbol{\Omega}_i - \mathbf{r}_{cj}\times\boldsymbol{\Omega}_j. \tag{16}$$

Here, $\mathbf{v}_i = \dot{\mathbf{x}}_i$ is the translational velocity of particle i, $\boldsymbol{\Omega}_i = \dot{\theta}_i$ its angular velocity, and $\mathbf{r}_{ci}$ is the vector from the centre of gravity of particle i to the contact point c. For spherical particles one has

$$\begin{aligned}\mathbf{r}_{ic} &\equiv \mathbf{r}_c - \mathbf{r}_i = -R_i\mathbf{n}_{ij},\\ \mathbf{r}_{cj} &\equiv \mathbf{r}_c - \mathbf{r}_j = R_j\mathbf{n}_{ij}.\end{aligned} \tag{17}$$

Here, R_i is the radius of particle i. It should be noted that the angular velocities $\boldsymbol{\Omega}_i$ and $\boldsymbol{\Omega}_j$ also have a component in the normal direction which causes the two particles to spin around the normal direction with velocity:

$$(\boldsymbol{\Omega}_i - \boldsymbol{\Omega}_j)\cdot\mathbf{n}_{ij}. \tag{18}$$

Contact forces originating from this component are usually ignored.

5.1. Normal contact forces

The normal component of the contact force acting on particle i is generally described as a function of the virtual overlap, ξ_{ij},

$$\delta n_{ij} = R_i + R_j - |\mathbf{x}_i - \mathbf{x}_j| \tag{19}$$

and its time derivative, $\dot{\xi}$,

$$\mathbf{F}_{in} = F_{in}(\xi_{ij}, \dot{\xi}_{ij})\mathbf{n}_{ij}. \tag{20}$$

By Newton's third law

$$\mathbf{F}_{jn} = -\mathbf{F}_{in}. \tag{21}$$

The simplest model assumes a linear elastic component and a linear viscous damping:

$$F_n(\xi, \dot{\xi}) = k_n\xi + \gamma_n\dot{\xi}. \tag{22}$$

Linear viscous damping leads to a normal contact force with a discontinuity at $\xi = 0$ where the force jumps from 0 to a finite value in an infinitely short time interval. The model is interesting because it has an analytic solution [64].

It has been shown [65–67], however, that for viscoelastic materials a non-linear model can be derived:

$$F_n(\xi, \dot{\xi}) = \tilde{k}_n\xi^{3/2} + \tilde{\gamma}_n\xi^{1/2}\dot{\xi}, \tag{23}$$

where the elastic constant $\tilde{k}_n$ and the damping constant $\tilde{\gamma}_n$ depend on Young's moduli, the Poisson ratios and bulk viscosities of the particles material, as well as on their masses and radii. The $\xi^{1/2}$ factor in the damping term makes the discontinuity at $\xi = 0$ disappear. Eq. (23), incorporates the special case of Hertz' contact law for purely elastic bodies, by setting the bulk viscosities of the particle's material to zero. It should be noted that Eq. (23) represents the analytic solution of simplified problem. The most important underlying assumptions are that the particles are

spherical and homogenous, deformations are small:

$$\xi/R \leqslant 0.01, \tag{24}$$

and the collision is head on, i.e., the particles approach each other along a line joining their centres of mass, and without rotation. During an oblique collision the normal component of the contact force can in principle deviate from Eq. (23) because of non-homogenous stress distributions at the contact surface. For agricultural products these assumptions are not always fullfilled. For example tomatoes are quite soft, allowing for larger deformation, and also not homogenous. For such systems little or no theoretical knowledge is available to build contact force models. An attempt to deal with large deformations has been reported by Raji and Favier [68].

5.2. Tangential contact forces

Tangential contact forces arise when two particles take part in an oblique collision or when the particles are rotating. The simplest tangential contact force model accounts for Coulomb friction only (see Eqs. (5) and (6)):

$$\mathbf{F}_\tau = -\mu|F_n|\boldsymbol{\tau}. \tag{25}$$

Note that Eq. (25) is discontinuous at $|\mathbf{v}| = 0$, which leads to F_τ jumping between positive and negative values rather than $F_r = 0$. This can be avoided by adding a viscous term

$$\mathbf{F}_\tau = -\min(\gamma_\tau\dot{\zeta}, \mu|F_n|)\boldsymbol{\tau}. \tag{26}$$

Here,

$$\zeta(t) = \int_{t_0}^{t} v_\tau(t')\mathrm{H}(\mu_d|F_n| - k_\tau|\zeta|)\mathrm{d}t' \tag{27}$$

plays a similar role as the virtual overlap ξ in normal contact force models. It is the displacement in the tangential direction that took place since the time t_0, when the contact was first established. Note that the Heaviside function

$$\mathrm{H}(x) = \begin{cases} 0 & \text{if } x < 0, \\ 1 & \text{if } x \geqslant 0 \end{cases} \tag{28}$$

takes care of keeping ζ constant in the regime of dynamic friction [69]. The friction factor μ in Eq. (26) switches back and forth between μ_s and μ_d whenever the border between static and dynamic friction regimes is crossed.

As for normal impact, realistically behaving tangential contact force models also require elastic terms:

$$\mathbf{F}_\tau = -\min(k_\tau\zeta + \gamma_\tau\dot{\zeta}, \mu|F_n|)\boldsymbol{\tau}. \tag{29}$$

Under the assumption of constant normal force Mindlin and Deresiewicz [70] were able to derive analytical results for purely elastic bodies. Their results where used by Walton and Braun [71] to derive an additive scheme for the elastic contribution of the tangential contact force:

$$\delta F_\tau = k_\tau|\delta\zeta|, \tag{30}$$

where, for any quantity q

$$\delta q \equiv q(t) - q(t - \delta t).$$

The tangential spring constant in Eq. (30) is given by

$$k_\tau = \begin{cases} k_\tau^0 \left(1 - \dfrac{F_\tau - F_\tau^*}{\mu F_n - F_\tau^*}\right)^{1/3} & \text{if } v_\tau \text{ in initial direction,} \\ k_\tau^0 \left(1 - \dfrac{F_\tau^* - F_\tau}{\mu F_n - F_\tau^*}\right)^{1/3} & \text{if } v_\tau \text{ in opposite direction,} \end{cases}$$

$$k_\tau^0 = k_n \frac{1 - v}{1 - v/2}, \tag{31}$$

where v is Poisson's ration for the particle's material. The quantity F_τ^* is initially equal to 0 and set to the current value of F_τ whenever v_τ reverses direction. The change in the normal force that inevitably occurs during impact is accounted for by using the instantaneous value of F_n in evaluating k_τ in Eq. (31).

6. Time integration

A numerical scheme for time integration is needed in order to solve the ODE system (1) numerically. To the knowledge of the authors very little systematic research has been done on numerical integration of DEM problems, mainly because numerical errors are considered less important than the approximate nature of the contact force models. For many DEM simulations, the reported integration time step is very often chosen to produce between 10 and 20 time steps over the timespan of a typical collision, often with low order integration schemes. However, Schäfer et al. [63] recommend 100 time steps and higher order integration schemes for accurate results. A comparative study of time integration algorithms for molecular dynamics has been published by Rodger [72].

Basic time marching methods are described by Ascher and Petzold [73], Golub and Ortega [74] and Lambert [75]. Implicit methods as well as adaptive multi-step methods are usually not considered in DEM because the improvement in accuracy comes at an excessively high cost caused by multiple contact detection phases per time step.

The forward Euler scheme

$$\begin{aligned} \mathbf{v}_{t+\Delta t} &= \mathbf{v}_t + \mathbf{a}_t \Delta t, \\ \mathbf{x}_{t+\Delta t} &= \mathbf{x}_t + \mathbf{v}_t \Delta t \end{aligned} \tag{32}$$

is only first order accurate, but simple to implement.

Many time integration schemes are borrowed from molecular dynamics [33,57], e.g. the *Verlet scheme* [76]:

$$\mathbf{x}_{t+1} = 2\mathbf{x}_t - \mathbf{x}_{t-1} + \Delta t^2 \mathbf{a}_t, \tag{33}$$

which is fourth order accurate. Unfortunately, it does not generate velocities directly. This is problematic in contact force models with damping since then the contact force depends on the

velocities of the colliding particles. Velocities can be provided as

$$\mathbf{v}_t = \frac{\mathbf{x}_t - \mathbf{x}_{t-\Delta t}}{\Delta t}, \tag{34}$$

which is only first-order accurate. Note that a central difference scheme

$$\mathbf{v}_t = \frac{\mathbf{x}_{t+\Delta t} - \mathbf{x}_{t-\Delta t}}{2\Delta t} \tag{35}$$

is not satisfactory as it makes the method implicit. In contact force models with damping the accelerations $\mathbf{a}_t = \mathbf{F}_t(\mathbf{x}_t, \mathbf{v}_t)/m$ depends on the velocities $\mathbf{v}_t$ and consequently, according to Eq. (35), also on the positions $\mathbf{x}_{t+\Delta t}$. This implies that contact detection needs to be executed more than once per time step, which is computationally too expensive. The *velocity Verlet scheme*

$$\begin{aligned} \mathbf{x}_{t+\Delta t} &= \mathbf{x}_t + \mathbf{v}_t \Delta t + \mathbf{a}_t \frac{\Delta t^2}{2}, \\ \mathbf{v}_{t+\Delta t} &= \mathbf{v}_t + \Delta t \frac{(\mathbf{a}_t + \mathbf{a}_{t+\Delta t})}{2}, \end{aligned} \tag{36}$$

does generate velocities but again becomes implicit in the case of contact force models with damping because of the appearance of the acceleration at the next time step, $\mathbf{a}_{t+\Delta t}$. which is dependent on the velocity at the next time step, $\mathbf{v}_{t+\Delta t}$. Here, however, $\mathbf{v}_{t+\Delta t}$ can be determined iteratively without doing contact detection at every iteration as the positions, $\mathbf{x}_{t+\Delta t}$, depend on the acceleration at the current time step, $\mathbf{a}_t$, only, and not on the acceleration at the next time step, $\mathbf{a}_{t+\Delta t}$. Another popular time integration method in MD is the leap-frog scheme:

$$\begin{aligned} \mathbf{v}_{t+\Delta t/2} &= \mathbf{v}_{t-\Delta t/2} + \mathbf{a}_t \Delta t, \\ \mathbf{x}_{t+\Delta t} &= \mathbf{x}_t + \mathbf{v}_{t+\Delta t/2} \Delta t. \end{aligned} \tag{37}$$

Here, velocities are only generated in the middle of the time steps, so that $\mathbf{v}_i$ must be extrapolated from $\mathbf{v}_{t-i\Delta t/2}$ $i = 1, 2, \ldots$. Beeman's algorithm [77] is fourth order accurate in $\mathbf{x}$ and third order accurate in $\mathbf{v}$ and has been reported to be particularly good at energy conservation in MD:

$$\begin{aligned} \mathbf{x}_{t+\Delta t} &= \mathbf{x}_t + \mathbf{v}_t \Delta t + \frac{\Delta t^2}{6}(4a_t - a_{t-\Delta t}), \\ \mathbf{v}_{t+\Delta t} &= \mathbf{v}_t + \frac{\Delta t}{6}(\mathbf{a}_{t+\Delta t} + 5\mathbf{a}_t - \mathbf{a}_{t-\Delta t}). \end{aligned} \tag{38}$$

Again in the case of contact force models with damping the appearance of $\mathbf{a}_{t+\Delta t}$ requires iterative determination of $\mathbf{v}_{t+\Delta t}$. Finally, also predictor-corrector methods have been used [57,63].

A problem that is most often simply ignored, is the fact that commonly used contact force models, based on linear damping (see Eq. (22)), are in fact discontinuous. Since the impact velocity is non-zero, the contact force jumps from 0 to a finite value in an infinitely small time, which is not only unphysical, but poses special problems to numerical solution methods [73]. Ideally, systems with discontinuous right hand sides require the discontinuity to be located so that a mesh point can be placed close to it. In the DEM problem this would require that the beginning of every contact be located in time. As there may be numerous contacts beginning and ending all the time, this is computationally very expensive. An alternative strategy is to use very small time steps near the discontinuities, which is of course also computationally expensive.

7. DEM applications in agriculture

Computer simulations of real problems have always been attractive because they provide a means of investigating model systems in order to gain understanding, and to conduct "computer" experiments in cases where experimental systems are hard to probe. This especially the case for granular systems where experiments with non-ideal materials are extremely hard to probe and a general theory is not available.

In this section a review of—still scarce—DEM applications for agricultural purposes is presented. Applications related to silo research is explicitly excluded, as this is already a well developed area, with many applications in other engineering disciplines. For recent results the reader is referred to Hirschfeld and Rapaport [78], de Silva [79], Holst et al. [80,81], Rotter et al. [82] Lu et al. [83], Negi et al. [84,85] and Rong et al. [86,87]. This overview is organized rather arbitrarily by distinguishing two different application domains: soft granular systems and hard granular systems. Soft granular systems of biological products are usually systems of fruits or tubers, like potatoes, tomatoes, apples, etc. with a rather small number of particles, but complex shapes. The main issue in the investigation of these systems is related to contact mechanics during collisions with other fruits or machine parts during harvesting and post-harvest treatment and its effect on material failure, such as bruising (e.g. potato, apple, pear, etc.) and puncturing (e.g. tomato). The aim is to design machines and process with a low risk of damaging the product. A lot of experimental work has been carried out to assess the mechanical behaviour of fruit upon impact and the related failure behaviour using pendulums [88–97,18].

These efforts have resulted in reliable techniques for measuring normal impact forces as a function of strain and strain rate during impact. However, little data are available on the measurement of tangential contact forces. Yet, it is suspected that e.g., during the harvesting of potatoes impacts with large tangential forces are an important source of bruise. A typical behaviour of a mealy apple upon mechanical impact by a spherical aluminium impactor of a pendulum is shown in Figs. 3 and 4. Note that the contact force returns to zero at a finite displacement, i.e., the contact ends before the apple surface has relaxed. Since the displacement rate is finite this implies that the relaxation is still going on but its rate is slower than the velocity

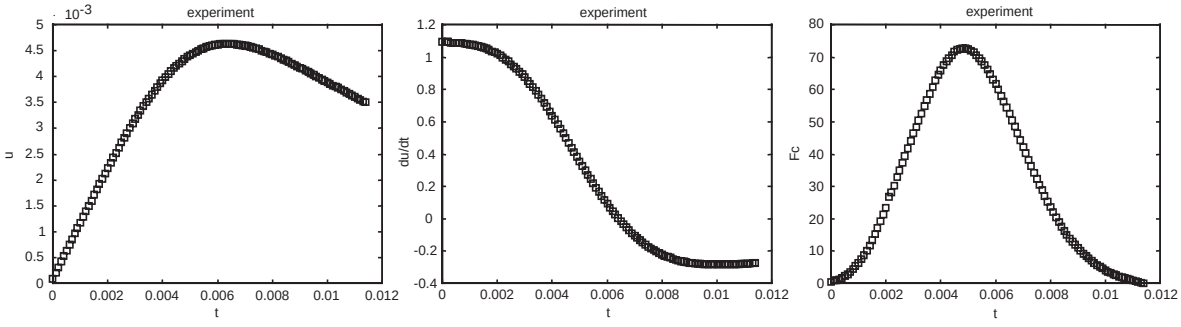

Fig. 3. Typical behaviour of a mealy apple impacted with a pendulum. The velocity at impact is 1.09 m/s which corresponds approximately with an initial angle of the pendulum of 25° (all units in S.I.). From left to right: displacement u of the impactor relative to the initial impact point, the displacement rate $\dot{u}$, and the force F_c exerted by the impacted object, i.e. the apple, on the impactor, as functions of time t.

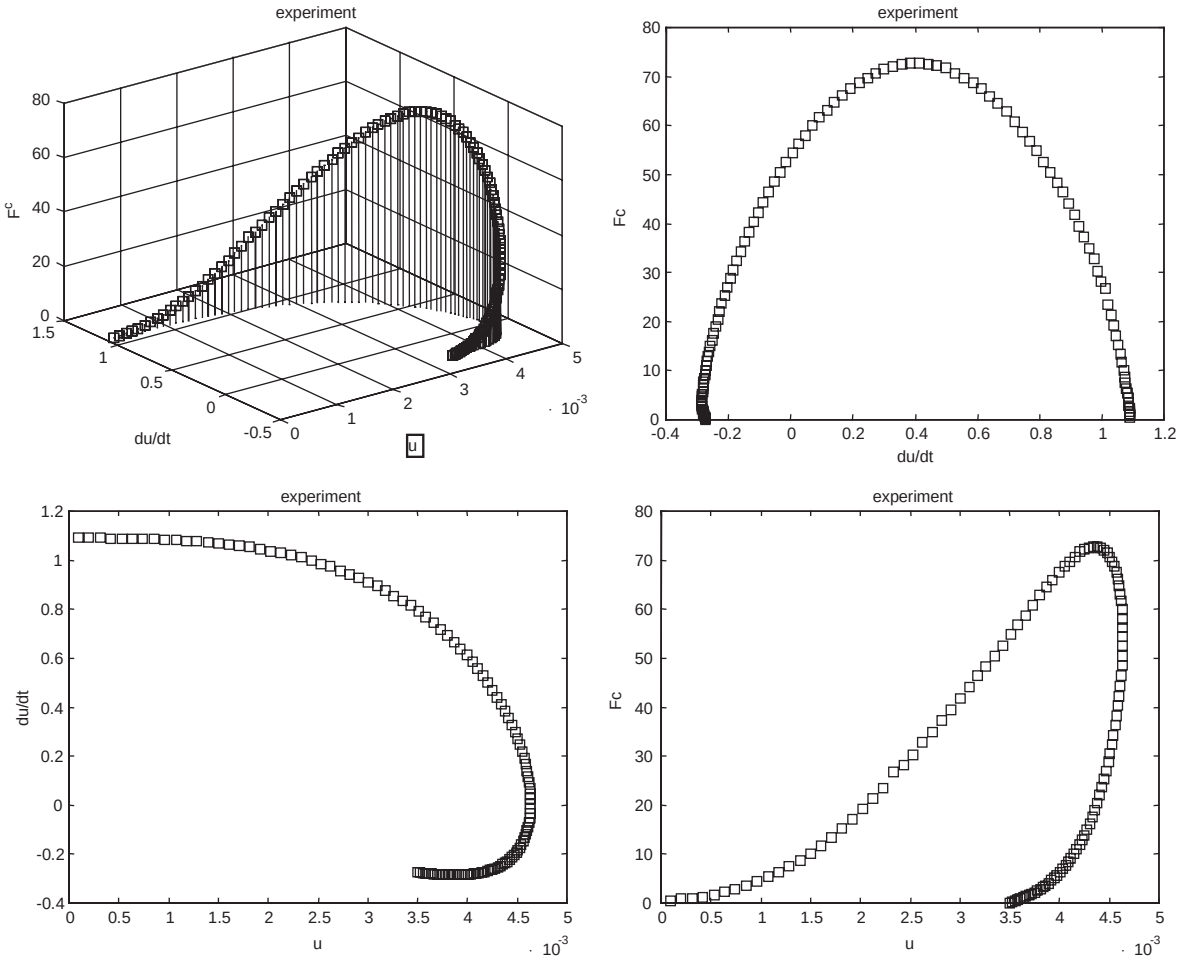

Fig. 4. Experimental contact force as a function of the trajectory in phase space $(u, \dot{u})$ and its different projections. Upper left: contact force as a function of the trajectory in phase space $(u, \dot{u})$ (time proceeds in clockwise orientation). Lower left: phase space trajectory (time proceeds in clockwise orientation). Upper right: force vs. displacement rate (time proceeds in counter-clockwise orientation). Lower right: force vs. displacement (time proceeds in clockwise orientation).

of the recoiling impactor (the displacement and displacement rate are inferred from the angular velocity of the impactor).

Fig. 5 shows a simulated impact using the Brilliantov model for the normal contact force, Eq. (23). Note the vertical slope of the contact force versus displacement curve at zero displacement which is not present in the experimental curve (Fig. 3). This singularity is caused by the presence of the $\xi^{1/2}$ factor in the damping term. Clearly, the apple is violating some of the assumptions of the Brilliantov model. Most probably, the mealy apple tissue is not an ideal visco-elastic solid, but it is also possible that the assumption of small deformation is violated. This illustrates clearly that, even for normal impacts, there is a lack of theoretical knowledge on

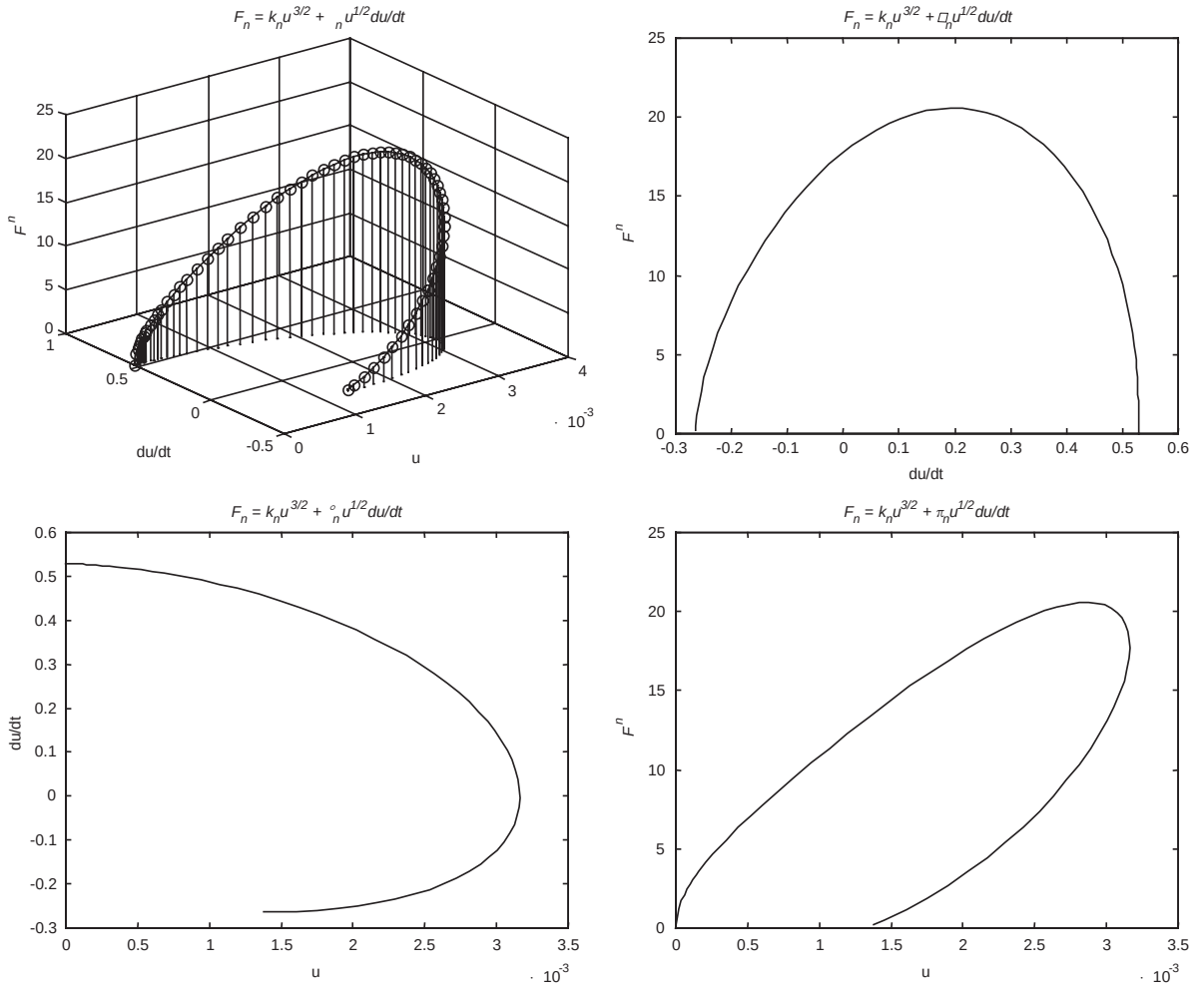

Fig. 5. A simulated impact using the Brilliantov model for the normal contact force. Note the vertical slope of the contact force vs. displacement curve.

contact force models for biological materials and more research is needed to link mechanical properties of biological materials to contact force models. Replacing the $\xi^{1/2}$ factor in the damping term by ξ gives a better qualitative agreement, as shown in Fig. 6. Now the slope at zero displacement is finite as experimentally observed. Contact force models like this can be fitted to experiments and used in DEM simulations to predict the bruise level in a particular harvester or post-harvest treatment. Typical examples are presented by Favier et al. [41] and Kremmer and Favier [42].

An entirely different case is the work of Schembri and Harris [98] who used DEM to describe the failure behaviour of sugar cane under compressive forces. Here, contact forces are taken to be cohesive bonds between cells. If the tensile forces between cells exceed the failure criterion the cells debond and the sugar cane splits.

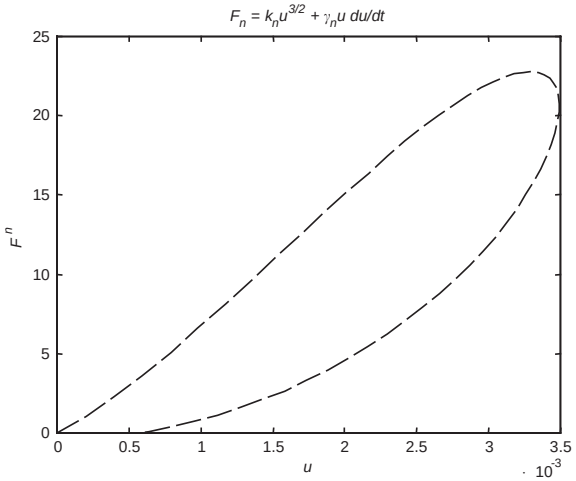

Fig. 6. A simulated contact force–displacement curve using the Brilliantov model for the normal contact force with the $\xi^{1/2}$ factor in the damping term replaced by ξ.

Hard granular systems of biological products usually consist of smaller particles and deal with flow or compaction problems. Technical difficulties, here, are mainly related to the large number of particles and adequate representation of irregular shapes without blowing up the contact detection phase. Here the approximation of bodies by overlapping spheres [41–43] has proven very useful. Typical problems treated are grains on a hopper [42], segregation of rice grains in a shaking tray [99], gravity flow of rice grains [100–102] and the prediction of bulk compression parameters of a compressed oil-seed bed [103]. Recently, DEM has been used to investigate the collective behaviour of mineral fertiliser grains in centrifugal fertiliser spreaders [88,104,105]. The ultimate goals of that study is to understand the interaction of fertiliser grains on the spreader disk, find out about the near-optimal fertiliser material properties, which guarantee a satisfactory spreading pattern, and to optimise the design of the spreader. Fig. 7 shows the simulated trajectory of a package of 144 spherical grains on a conical disk.

8. Conclusions

The numerical simulation of granular systems of biological products is a complex task that requires DEM techniques at the limit of what is technically possible today. They show irregular shapes, not necessarily convex. They exhibit material properties that often differ from ideal solids like viscoelastic materials and are hard to assess. There is biological variability of mechanical properties among different specimens of the product, but also within a single specimen. Failure properties of the material (like bruise or puncturing) are often essential. 3D simulations are required. Yet, interesting applications are emerging, providing interesting insights into the mechanical behaviour of biological products and helping to design better tools for material handling. It should be clear from the discussion that quite a number of issues are yet to be

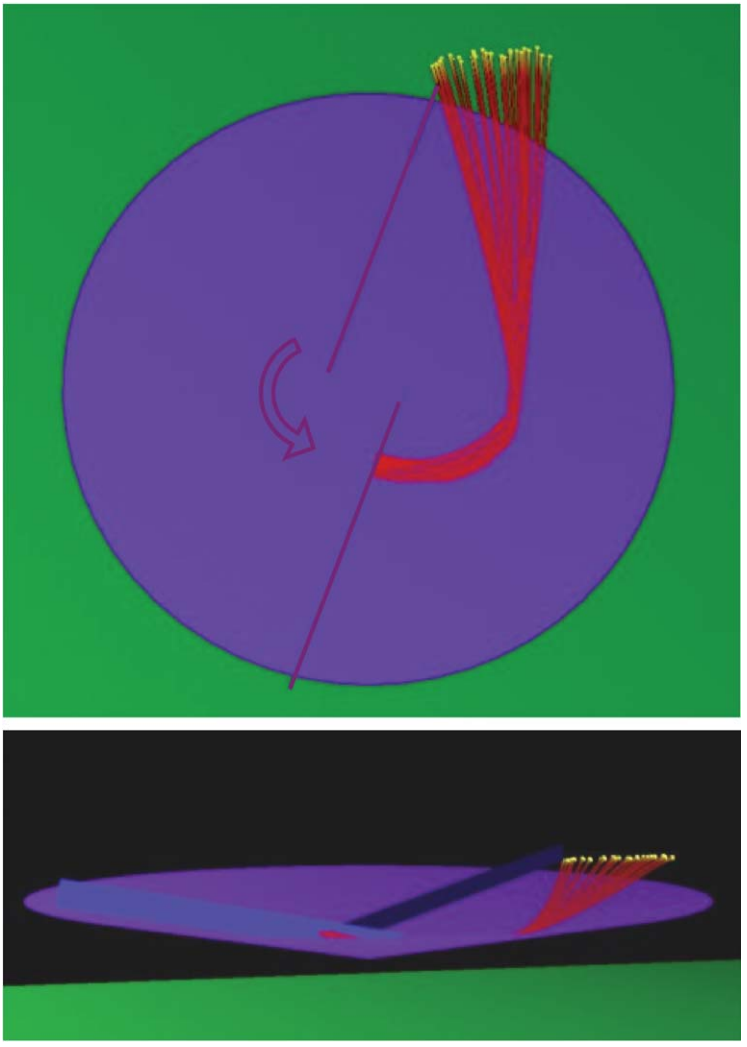

Fig. 7. Simulation of the trajectory of 144 particles falling on a spinning conical disk with two vanes. Above: Top view of the trajectory of the particles. Below: side view. The motion of the vanes on the disk is not shown.

resolved before DEM can become interesting on an industrial scale. Efficient computational methods are needed for representing irregular forms. Basic research is required to enlighten the link from the mechanical and micro-mechanical properties of biological products to contact force models. Finally, as DEM covers a wide range of applications with different numbers of particles, different particle shapes, differing contact physics simulations a computational framework for developing is needed for efficiently building new DEM applications. Current software systems very often have a very restricted application range. An attempt to cope with this problem is the DEMeter++ project [106]. DEMeter++ is a C++ class library in development that is to be used as an extensible toolkit for efficient development of high performance DEM applications using state of the art algorithms and scientific programming techniques. The central idea is a

building brick approach in which all the components, like shape representation, contact forces, spatial sorting, spatial resolution, time integration, etc. in the basic DEM algorithm become separate objects which can be easily interchanged and extended or replaced by user-defined objects.

References

[1] S.C. Cowin, M. Satake, *Proceedings of the US/Japan Seminar on Continuum Mechanical and Statistical Approaches in the Mechanics of Granular Materials*, Gakujutsu Bunken Fukyu-kai, Tokyo, 1978.
[2] P.A. Vermeer, H.J. Luger, *IUTAM Symposium on Deformation and Failure of Granular Materials*, Balkema, Rotterdam, 1982.
[3] J.T. Jenkins, M. Satake, *Proceedings of the US/Japan Seminar on New Models and Constitutive Relations in the Mechanics of Granular Materials*, Elsevier, Amsterdam, 1983.
[4] M. Satake, J.T. Jenkins, *Proceedings of the US/Japan Seminar on Micromechanics of Granular Matter*, Elsevier, Amsterdam, 1988.
[5] M. Satake, Mechanics of Granular Materials, Report of ISSMFE Technical Committee on Mechanics of Granular Material, The Japanese Geotechnical Society, Tokyo, 1989.
[6] J. Biarez, R. Gourvés, *Powders & Grains 89, Proceedings of the International Conference on Micromechanics of Granular Media*, Balkema, Rotterdam, 1989.
[7] D. Bideau, A. Hansen, *Disorder and Granular Media, Random Materials and Processes*, North-Holland, Amsterdam, 1993.
[8] C. Thornton, *Powders & Grains 93, Proceedings of the Second International Conference on Powders & Grains*, Balkema, Rotterdam, 1993.
[9] N.A. Fleck, A.C.F. Cocks, *IUTAM Symposium on Mechanic of Granular and Porous Materials*; Cambridge, UK, 15–17 July 1996, Kluwer Academic Publishers, Dordrecht, 1997.
[10] R.P. Behringer, J.T. Jenkins (Eds.), *Powders & Grains 97*, *Proceedings of the Third International Conference on Powders & Grains*, AA Balkema, Rotterdam, 1997.
[11] C.S. Chang, A. Misra, T.Y. Liang, M. Babic, *Mechanics of Deformation and Flow of Particulate Materials*, American Society of Civil Engineers, New York, 1997.
[12] P. Middleton, Taking a bite from your profits?, *Bulk Handling International* (1997) 39–40.
[13] J. Duran, *Sands, Powders and Grains: An Introduction to the Physics of Granular Materials*, Springer, Berlin, 2000.
[14] B.J. Ennis, J. Green, R. Davis, *Particle Technology* 90 (1994) 32.
[15] T.M. Knowlton, J.W. Carson, E. Klinzing, W.-C. Yang, *Particle Technology* 90 (1994) 44.
[16] R. Bartram, J. Fountain, K. Olsen, D. O'Rourke, Washington state apple condition at retail, 1982–83, *Proceedings of the Washington State Horticultural Society* 79 (1983) 36–46.
[17] M. Baheri, Development of a Method for Prediction of Potato Mechanical Damage in the Chain of Mechanized Potato Production, Ph.D. Thesis, Faculty of Agricultural and Applied Biological Sciences, KULeuven, 1997.
[18] G.-J. Molema, Mechanical Force and Subcutaneous Tissue Discoloration in Potato, Ph.D. Thesis, Wageningen Universiteit, 1999.
[19] M. Oda, K. Iwashita, *Mechanics of Granular Materials*, A.A. Balkema, Rotterdam, 1999.
[20] H.M. Jaeger, S.R. Nagel, R.P. Behringer, Granular solids, liquids and gases, *Reviews of Modern Physics* 68 (1996) 1259–1273.
[21] H.M. Jaeger, S.R. Nagel, R.P. Behringer, The physics of granular materials, *Physics Today* (1996) 32–38.
[22] D. Kestenbaum, Sand castles and cocktail nuts, *New Scientist* (1997) 25–28.
[23] J.R. Williams, R. O'Connor, Discrete element simulation and the contact problem, *Archives of Computational Methods in Engineering* 6 (4) (1999) 279–304.
[24] J.R. Williams, R.M. O'Connor, A linear complexity intersection algorithm for discrete element simulation of arbitrary geometries, *Engineering Computations* 12 (1995) 85–201.

[25] J.-A. Ferrez, D. Müller, T.M. Liebling, Parallel implementation of a distinct element method for granular media simulation on the cray T3D, EPFL, *Supercomputing Review* 8 (1996) 4–7.
[26] J.-A. Ferrez, Th.M. Liebling, D. Müller, Dynamic triangulations for granular media simulations, in: K. Mecke, D. Stoyan (Eds.), *Statistical Physics and Spatial Statistics*, Springer, Berlin, 1999.
[27] P.W. Cleary, N. Stokes, J. Hurley, Efficient collision detection for three dimensional super-ellipsoid particles, in: *Proceedings of the Eighth International Computational Techniques and Applications Conference*, World Scientific, 1997.
[28] H. Laux, Modeling of Dilute and Dense Dispersed Fluid-particle Two-phase Flows, Ph.D. Thesis, Norwegian University of Science and Technology, 1998.
[29] M.L. Sawley, P.W. Cleary, A parallel discrete element method for industrial granular flow simulations, *EPFL Supercomputing Review* 11 (1999) 23–29.
[30] T. Iwai, C.W. Hong, P. Greil, Fast particle pair detection algorithms for particle simulations, *International Journal of Modern Physics C* 10 (1999) 823–837.
[31] P.A. Cundall, O.D.L. Strack, A discrete numerical model for granular assemblies, *Géotechnique* 29 (1979) 47–65.
[32] P.A. Cundall, A discontinuous future for numerical modelling in geomechanics?, *Proceedings of the Institution of Civil Engineers-Geotechnical Engineering* 149 (2001) 41–47.
[33] D.C. Rapaport, *The Art of Molecular Dynamics Simulation*, Cambridge University Press, Cambridge, 1997.
[34] M.C. Lin, S. Gottschalk, Collision detection between geometric models: a survey, in: *Proceedings of IMA Conference on Mathematics of Surfaces 1998*, 1998.
[35] M.C. Lin, D. Manocha, Fast interference detection between geometric models, *The Visual Computer* 11 (1995) 542–561.
[36] G. Farin, *Curves and surfaces for Computer Aided Design: A Practical Guide*, Academic Press Inc., New York, 1993.
[37] J.M. Lane, R.F. Riesenfeld, A theoretical development for the computer generation and display of piecewise polynomial surfaces, *IEEE Transactions on Pattern Analysis and Machine Intelligence* 2 (1) (1980) 150–159.
[38] S. Gottschalk, Collision Queries Using Oriented Bounding Boxes, Ph.D. Thesis, University of North Carolina, 2000.
[39] J.T. Klosowski. Efficient Collision Detection for Interactive 3D Graphics and Virtual Environments, Ph.D. Thesis, State University of New York, 1998.
[40] M.C. Lin, Efficient Collision Detection for Animation and Robotics, Ph.D. Thesis, University of California, Berkeley, 1993.
[41] J.F. Favier, M.H. Abbaspour-Fard, M. Kremmer, A.O. Raji, Shape representation of (axisymmetrical), non-spherical particles in discrete element simulation using multi-element model particles, *Engineering Computations: International Journal for CAE and Software* (1999).
[42] M. Kremmer, J.F. Favier, Multi-body dynamics simulation using ReDem (the Reverse engineered Discrete Element Method), in: *Proceedings of ASAE International Conference*, 1999.
[43] M.H. Abbaspour, A.O.Raji, J.F. Favier, Discrete element modelling of the flow of irregularly shaped particulate agricultural materials, in: *EurAgEng 98*, paper 98-F-57, 1998.
[44] C. Hogue, Shape representation and contact detection for discrete element simulations of arbitrary geometries, *Engineering Computations* 15 (1998) 374.
[45] R.M. O'Connor, A Distributed Discrete Element Modelling Environment—Algorithms, Implementation and Applications, Ph.D. Thesis, MIT, 1996.
[46] A. Gregory, M.C. Lin, S. Gottschalk, R. Taylor, Fast and accurate collision detection for haptic interaction using a three degree-of-freedom force-feedback device, *Computational Geometry—Theory and Applications* 15 (2000) 69–89.
[47] J.T. Klosowski, M. Held, J.S.B. Mitchell, H. Sowizral, K. Zikan, Efficient collision detection using bounding volume hierarchies of k-DOPs, *IEEE Transactions on Visualization and Computer Graphics* 4 (1998).
[48] S. Krishnan, M. Gopi, M.C. Lin, D. Manocha, A. Pattekar, Rapid and accurate contact determination between spline models using shelltrees, in: *Proceedings of Eurographics'98*, 1998.

[49] S. Krishnan, A. Pattekar, M.C. Lin, D. Manocha, Spherical Shell: A higher order bounding volume for fast proximity queries, in: *Proceedings of WAFR'98*, 1998.
[50] T. Hudson, M.C. Lin, J. Cohen, S. Gottschalk, D. Manocha, V-COLLIDE: Accelerated collision detection for VRML in: *Proceedings of VRML'97*, 1997.
[51] J. Cohen, M. Lin, D. Manocha, K. Ponamgi, I-COLLIDE: An interactive and exact collision detection system for large-scaled environments, in: *Proceedings of ACM International 3D Graphics Conference*, 1995.
[52] M. Held, J.T. Klosowski, J.S.B. Mitchell, Evaluation of collision detection methods for virtual reality fly-throughs, in: *Proceedings of the Seventh Canadian Conference on Computational Geometry*, 1995.
[53] A. Garcia-Alonso, N. Serrano, J. Flaquer, Solving the collision detection problem, *IEEE Computer Graphics and Applications* 14 (1994) 36–43.
[54] V. Buchholtz, T. Pöschel, A vectorized algorithm for molecular-dynamics of short-range interacting particles, *International Journal of Modern Physics C* 4 (1993) 1049–1057.
[55] W. Form, N. Ito, G.A. Kohring, Vectorized and parallelized algorithms for multimillion particle md-simulation, *International Journal of Modern Physics C* 4 (1993) 1085–1107.
[56] R.W. Hockney, J.W. Eastwood, *Computer Simulation Using Particles*, McGraw-Hill, New York, 1981.
[57] M.P. Allen, D.J. Tildesley, *Computer Simulation of Liquids*, Clarendon, Oxford, 1999.
[58] M. Vankreveld, M. Overmars, P. Agarwal, Intersection queries in sets of disks, *BIT* 32 (1992) 268–279.
[59] M. Moore, J. Wilhelms, Collision detection and response for computer animation, *Computer Graphics (SIGGRAPH'88 Proceedings)* 22 (1988) 289–298.
[60] H. Noborio, S. Fukuda, S. Arimoto, Fast interference check method using octree representation, *Advanced Robotics* 3 (1989) 193–212.
[61] D. Müller, Techniques Informatiques Efficaces pour la Simulation de Milieux Granulaires par des Methodes d'Éléments Distincts, Ph.D. Thesis, Ecole Polytechnique Fédérale de Lausanne, 1996.
[62] R. Sedgewick, *Algorithms in C*, Addison-Wesley, Reading, MA, 1990.
[63] J. Schäfer, S. Dippel, D.E. Wolf, Force schemes in simulations of granular materials, *Journal de Physique I France* 6 (1996) 5–20.
[64] D. Zhang, W.J. Whiten, The calculation of contact forces between particles using spring and damping models, *Powder Technology* 88 (1996) 59–64.
[65] N.V. Brilliantov, F. Spahn, J. Hertzsch, T. Pöschel, Model for collisions in granular gases, *Physical Review E* 53 (1996) 5382–5392.
[66] T. Schwager, T. Pöschel, Contact of viscoelastic spheres, in: D.E. Wolf, P. Grassberger (Eds.), *Friction, Arching, Contact Dynamics*, World Scientific, Singapore, 1996.
[67] G. Kuwabara, K. Kono, Restitution coefficient in a collision between 2 spheres, *Japanese Journal of Applied Physics* 26 (8) (1987) 1230–1233.
[68] A.O. Raji, J.F. Favier, Discrete Element Modelling of deformation in particulate agricultural materials under bulk compressive loading, in: *EurAgEng 98*, Paper 98-F-045, 1998.
[69] L. Brendel, S. Dippel, Lasting contacts in molecular dynamics simulations, in: H.J. Herrmann, J.-P. Hovi, S. Luding (Eds)., *Physics of Dry Granular Materials*, NATO ASI Series E, Vol. no. 350, Kluwer, Dordrecht, 1998, pp. 313–318.
[70] R.D. Mindlin, H. Deresiewicz, Elastic spheres in contact under varying oblique forces, *American Society of Mechanical Engineers, Journal of Applied Mechanics* 20 (1953) 327–344.
[71] O. Walton, R. Braun, Viscosity, granular temperature, and stress calculations for spherical particles accounting for plastic deformation, *Journal of Rheology* 30 (1986) 949–980.
[72] P.M. Rodger, On the accuracy of some common molecular dynamics algorithms, *Molecular Simulation* 15 (1989) 263–269.
[73] U.M. Ascher, L.R. Petzold, *Computer Methods for Ordinary Differential Equations and Differential-Algebraic Equations*, SIAM, Philadelphia, 1998.
[74] G.H. Golub, J.M. Ortega, *Scientific Computing and Differential Equations: An Introduction to Numerical Methods*, Academic Press, New York, 1991.
[75] J.D. Lambert, *Numerical Methods for Ordinary Differential Systems*, Wiley, New York, 1991.

[76] L. Verlet, Computer experiments on classical fluids, I. Thermodynamical properties of Lennard-Jones molecules, *Physical Review* 159 (1967) 98–103.
[77] D. Beeman, Some multistep methods for use in molecular dynamics calculations, *Journal of Computational Physics* 20 (1976) 130–139.
[78] D. Hirsfeld, D.C. Rapaport, Granular flow from a silo: discrete-particle simulations in three dimensions, *European Physical Journal E* 4 (2001) 193–199.
[79] E. de Silva (Ed). *Proceedings of the International Symposium on Reliable Flow of Particulate Solids III (RELPOWFLO III)*, Telemark College, Porsgrunn, Norway, 1999.
[80] J.F.M.G. Holst, J.Y. Ooi, J.M. Rotter, G.H. Rong, Numerical modeling of silo filling: I Continuum analyses, *Journal of Engineering Mechanics-American Society of Civil Engineers* 125 (1999) 94–103.
[81] J.F.M.G. Holst, J.M. Rotter, J.Y. Ooi, G.H. Rong, Numerical modeling of silo filling: II Discrete element analyses, *Journal of Engineering Mechanics-American Society of Civil Engineers* 125 (1999) 104–110.
[82] J.M. Rotter, J.M.F.G. Holst, J.Y. Ooi, A.M. Sanad, Silo Pressure predictions using discrete-element and finite-element analyses, *Philosophical Transactions of the Royal Society of London Series A—Mathematical Physical and Engineering Sciences* 356 (1998) 2685–2712.
[83] Z. Lu, S.C. Negi, J.C. Jofriet, A numerical model for flow of granular materials in silos, Part 1: model development, *Journal of Agricultural Engineering Research* 68 (1997) 223–229.
[84] S.C. Negi, Z. Lu, J.C. Jofriet, A numerical model for flow of granular materials in silos, Part 2: Model validation, *Journal of Agricultural Engineering Research* 68 (1997) 231–236.
[85] S.C. Negi, Z. Lu, J.C. Jofriet, A numerical model for flow of granular materials in silos. Part 3: Parametric study, *Journal of Agricultural Engineering Research* 68 (1997) 237–246.
[86] G.H. Rong, S.C. Negi, J.C. Jofriet, Simulation of flow behaviour of bulk solids in bins, Part1: Model development and validation, *Journal of Agricultural Engineering Research* 62 (1995) 247–256.
[87] G.H. Rong, S.C. Negi, J.C. Jofriet, Simulation of flow behaviour of bulk solids in bins, Part 2: Shear bands, flow corrective inserts and velocity profiles, *Journal of Agricultural Engineering Research* 62 (1995) 257–269.
[88] E. Tijskens, P. Jancsok, M. Van Zeebroeck, Veerle Vanlinden, P. Van Liedekerke, H. Ramon, J. De Baerdemaeker, DEM modelling of agricultural processes: an overview of recent projects, in: P.-O. Gutman (Ed.), *Proceedings of the Fourth International Conference on Mathematical Modelling and Simulation in Agro- and Bio-Industries*, Haifa (Israel), June, 12–14, 2001.
[89] A.L. Baritelle, G.M. Hyde, Commodity conditioning to reduce impact bruising, *Postharvest Biology and Technology* 211 (3) (2001) 331–339.
[90] A.L. Baritelle, G.M. Hyde, Effect of tuber size on failure properties of potato tissue, *Transactions of the ASAE* 42 (1) (1999) 159–161.
[91] S. Gan-Mor, N. Galili, Rheological model for fruit collision with an elastic plate, *Journal of Agricultural Engineering Research* 75 (2000) 139–147.
[92] G. Wormanns, T. Hoffmann, A. Jacobs, Zur Bestimmung der Stossbelastung un Schwarzfleckigkeit bei Kartoffeln, *LandTechnik* 1 (2001) 32–33.
[93] R.W. Bajema, G.M. Hyde, Instrumented pendulum for impact characterization of whole fruit and vegetable specimens, *Transactions of the ASAE* 41 (5) (1998) 1399–1405.
[94] R.W. Bajema, G.M. Hyde, Packing line bruise evaluation for walla-walla summer sweet onions, *Transactions of the ASAE* 38 (4) (1995) 1167–1171.
[95] R.W. Bajema, G.M. Hyde, A.L. Baritelle, Temperature and strain rate effects on the dynamic failure properties of potato tuber tissue, *Transactions of the ASAE* 41 (3) (1998) 733–740.
[96] M., Geyer, B. Herold, C.J. Studman, Fruit contact pressure distributions, *EurAgEng*, Paper 98-F-001.
[97] R. Mathew, G.M. Hyde, Potato impact damage thresholds, *Transactions of the ASAE* 40 (3) (1997) 705–709.
[98] M.G. Schembri, H.D. Harris, Modelling impact on a biological material (sugar cane) using the discrete element method, *AgEng 96*, Madrid, Paper 96F-072, 1996.
[99] Sakaguchi, E., Kawakami, S., Suzuki, M., Urakawa, T., Favier, J.F., Effective use of DEM simulation for development of grain processing technology, in: *EurAgEng* 98 (1998).
[100] E. Sakaguchi, J.F. Favier, Analysis of the shear behaviour of a grain assembly using DEM simulation, *International Agrophysics* 14 (2000).

[101] E. Sakaguchi, J.F. Favier, Analysis of the shear behaviour of a grain assembly using DEM simulation, in: ICPAFP'98, *International Conference on Physics of Agro- and Food Products*, 1998.
[102] E. Sakaguchi, S. Kawakami, F. Tobita, Simulation on flowing phenomena of grains by distinct element method, in: *AgEng* '94, 1994.
[103] A.O. Raji, F.J. Favier, Discrete element modelling of the compression of an oil-seed bed, in: *Proceedings of the ASAE International Conference*, Paper 996109, 1999.
[104] R. Olieslagers, H. Ramon, J. De Baerdemaeker, Calculation of fertilizer distribution patterns from a spinning disc spreader by means of a simulation model, *Journal of Agricultural Engineering Research* 63 (1996) 137–152.
[105] J. Loodts, De Discrete Elementen methode voor de simulatie van korrelstromen, Eindwerk Bio-ingenieur in de Landbouwkunde, Faculty of Applied Biological and Agricultural Sciences, Catholic University Leuven, Belgium, 2001 (in Dutch).
[106] E. Tijskens, H. Ramon, J. De Baerdemaeker, DEMeter++: Development of an object oriented extensible toolkit for efficient DEM simulation, in: P.-O. Gutman (Ed.), *Proceedings of the Fourth International Conference on Mathematical Modelling and Simulation in Agro- and Bio-Industries*, Haifa, Israel, June, 12–14, 2001.